Biochemical and Biophysical Research Communications 422 (2012) 436–441

Contents lists available at SciVerse ScienceDirect

Biochemical and Biophysical Research Communications

journal homepage: www.elsevier.com/locate/ybbrc

Menthol induces cell-cycle arrest in PC-3 cells by down-regulating G2/M genes, including polo-like kinase 1

Su-Hwa Kim [a,1], Sanghoon Lee [b,1], Stephen R. Piccolo [c,d], Kristina Allen-Brady [e], Eun-Jung Park [a], Jung Nyeo Chun [a,f], Tae Woo Kim [g], Nam-Hyuk Cho [h], In-Gyu Kim [h], Insuk So [a,h,f], Ju-Hong Jeon [a,f,h,*]

[a] Department of Physiology, Seoul National University College of Medicine, Seoul 110-799, Republic of Korea
[b] Department of Biomedical Informatics, University of Utah, Salt Lake City, Utah 84112, USA
[c] Department of Pharmacology and Toxicology, University of Utah, Salt Lake City, Utah 84112, USA
[d] Division of Computational Biomedicine, Boston University School of Medicine, Boston, MA 02118, USA
[e] Department of Medicine, Division of Genetic Epidemiology, University of Utah, Salt Lake City, Utah 84112, USA
[f] Institute of Dermatological Science, Medical Research Center, Seoul National University, Republic of Korea
[g] Division of Oncology, Graduate School of Medicine, Korea University, Seoul 136-701, Republic of Korea
[h] Department of Biomedical Sciences, Seoul National University College of Medicine, Seoul 110-799, Republic of Korea

ARTICLE INFO

Article history:
Received 27 April 2012
Available online 9 May 2012

Keywords:
DNA microarray
Prostate cancer
Menthol
Gene set enrichment analysis
PLK1

ABSTRACT

Menthol, a naturally occurring monoterpene, is used in foods, cosmetic products, and topical therapeutic preparations. It also exerts cytotoxic activity against several cancer cell types, including prostate cancer cells. However, little is known about the mechanism of menthol action against prostate cancer cells. In this study, we investigated the effect of menthol on the gene expression profile of PC-3 prostate cancer cells using DNA microarray analyses. Gene set enrichment analysis revealed that menthol primarily affects the expression of cell cycle-related genes. Subsequent experimental analyses validated that menthol induces G2/M arrest. Particularly, menthol markedly down-regulated polo-like kinase 1 (PLK1), a key regulator of G2/M phase progression and inhibited its downstream signaling. Our computational analyses and experimental validation provide a basis for future investigations that are aimed at elucidating the action of menthol on cell cycle control in prostate cancer cells.

1. Introduction

Prostate cancer is one of the leading causes of cancer death among men in the world [1,2]. Androgen deprivation therapy is initially effective at controlling metastatic prostate cancer [3,4]. However, most metastatic prostate cancers relapse and progress into castration-resistant prostate cancer (CRPC) that is currently incurable due to lack of effective treatments [4,5]. Several studies have utilized gene-expression profiling in prostate cancer tissue to reveal gene signatures of metastatic progression or to predict the recurrence of aggressive prostate cancer [6–11]. In conjunction, further gene-expression profiling studies in cell lines, such as CRPC model cells, using anticancer reagent treatments are important to develop therapeutic strategies and identify treatment targets [12,13].

Menthol is a naturally occurring monoterpene found in the essential oil of members of the *Mentha* genus [14]. It has been widely used in foods, cosmetic products, and topical therapeutic preparations, where it is an active ingredient of cooling and flavoring and is used in antipruritic and analgesic formulations [14]. Menthol also exerts cytotoxic activity against several cancer cell types [15], including prostate cancer cells [16], although the molecular mechanism is not understood [14–16]. Understanding the biological processes of menthol that underlie its cytotoxic activity may lead to improved treatment strategies for CRPC.

Through an objective, genome-wide analysis, gene-expression profiling can provide a foundation for discovering the cellular response to growth inhibition in CRPC. In this study, we performed microarray experiments on PC-3 prostate cancer cells in order to obtain a global view of how menthol affects prostate cancer biology.

2. Material and methods

2.1. Cell culture and reagents

PC-3 cells were supplied by ATCC and maintained under DMEM medium containing 10% FBS. All cell culture agents used were

Abbreviations: PLK1, polo-like kinase 1; GSEA, gene set enrichment analysis; γTuRC, γ-tubulin ring complex; CRPC, castration-resistant prostate cancer.

* Corresponding author at: Department of Physiology and Biomedical Sciences, Seoul National University College of Medicine, 103 Daehak-ro, Jongno-gu, Seoul 110-799, Republic of Korea. Fax: +82 2 763 9667.
E-mail address: jhjeon2@snu.ac.kr (J.-H. Jeon).

[1] These authors contributed equally to this work.

0006-291X/$ - see front matter © 2012 Elsevier Inc. All rights reserved.
http://dx.doi.org/10.1016/j.bbrc.2012.05.010

obtained from Invitrogen. All other reagents not specified were supplied by Sigma-Aldrich. Menthol was dissolved in ethanol as a vehicle. The working concentration of ethanol was adjusted to 0.1%.

2.2. RNA isolation and microarray processing

Total RNA was extracted from PC-3 cells following treatment with either the vehicle or menthol at 1 mM for 24 h and then processed according to the manufacturer's guideline (Affymetrix). The extracted RNA was analyzed on an Agilent 2100 Bioanalyzer (Agilent Technologies) for RNA quality. All samples showed high RNA Integrity Number values >9.0 and 28S/18S ratios >1.5 [17,18]. RNA extract with A260/A280 and A260 absorbance ratio ranging from 1.8 to 2.1 was used for cDNA synthesis. The Affymetrix GeneChip® procedure was used for generating the biotin-labeled single-stranded cRNA from 300 ng total RNA by *in vitro* transcription (GeneChip® Whole Transcript (WT) Sense Target Labeling Assay Rev.5). Following fragmentation, 5.5 μg of fragmented cDNA were hybridized for about 17 h at 45 °C on Human Gene 1.0 ST arrays. Quality-control tests were applied to all microarrays using the pipeline at http://www.arrayanalysis.org. All samples had a normalized unscaled standard error score <1.1, relative log expression (RLE) score <0.1, and RLE interquartile range <1 in probe-set homogeneity tests [19,20]. No outlier samples were observed on RNA degradation plots [21].

Our raw data are available through the Gene Expression Omnibus (GEO) database (http://www.ncbi.nlm.nih.gov/geo) under accession no. GSE28241. Raw data were normalized using the Robust Multichip Average (RMA) method [22,23]. As part of the normalization process, a custom chip-definition file from the BrainArray resource was used to map microarray probes to 19,741 genes [24]. This annotation method reassigns probes to genes based on updated genome mappings and excludes inaccurate or wrongly annotated probes.

2.3. Computational analysis and statistics: unsupervised hierarchical clustering and GSEA

Unsupervised hierarchical clustering was used to group samples and genes that had similar expression values; Pearson correlation coefficients were used as column and row distances, and the pairwise complete-linkage method was used to construct the hierarchies. Then to enable visual inspection of the data, a heat map was generated using the GenePattern v3.2.3 software [25].

To identify genes that were expressed differentially between menthol- and vehicle-treated PC-3 cells, we applied Significance Analysis of Microarrays (SAM) [26]. SAM identifies statistically significant genes through use of gene specific *t*-tests; significance is determined by permutation testing to allow for correlation between genes and to avoid the necessity of meeting parametric assumptions. To correct for multiple testing, SAM also estimates a false discovery rate (FDR). We estimated our empirical null distribution using 1000 permutations and used an FDR threshold (*q*-value) of 0.05.

To enable better biological interpretation of the selected genes, gene-set enrichment analysis (GSEA) was applied to the data [27]. This method uses previously identified lists of genes that share a common biological theme (gene sets) and analyzes gene-expression patterns to identify gene sets that are coordinately up- or down-regulated. Gene sets that are "significantly enriched" can then be examined in more depth and used to aid in interpreting a list of selected genes. For this study, the Gene Ontology Biological Process (version 3.0) gene sets were used. Since the number of samples was small in this study, *p*-values were calculated by permuting the data 1000 times in the process of finding up- or down-regulated gene sets, and FDRs were calculated to adjust *p*-values for multiple hypothesis testing. Gene sets that were up- or down-regulated with a *q*-value <0.20 were considered significant. The GSEA software also provides an enrichment score (ES), which indicates the strength of the relationship between gene sets and phenotypes. Enrichment scores can be normalized (NES) to account for the size of each gene set. Negative ES values indicate that a gene set is down-regulated.

In addition to identifying enriched gene sets, the GSEA method also enables researchers to examine individual gene sets to determine which genes contribute most to a given ES; such genes are termed the *leading-edge subset* (LES). Examining LES can shed additional light on the distinct expression patterns behind particular biological processes—in this case, the processes that differ between menthol- and vehicle-treated cells. Not all members of a gene set will typically affect and participate in a biological process [28].

2.4. RT-PCR analysis

RT-PCR of β-actin was performed as previously described [29]. RT-PCR of PLK1 mRNA was performed using a forward primer (GGCAACCTTTTCCTGAATGA) and a reverse primer (AATGGACCACACATCCACCT). The following conditions were used for PCR: preheating (94 °C, 2 min), 35 cycles of denaturation (94 °C, 30 sec), annealing (50 °C, 30 sec), extension (72 °C, 60 sec), and final extension (72 °C, 10 min).

2.5. Quantitative real-time RT-PCR analysis

Real-time PCR was performed on a Step One Real-Time PCR System (Applied Biosystems) using Power SYBR Green PCR Master Mix (Applied Biosystems). Quantitative real-time PCR of PLK1 mRNA was performed using a forward primer (AACGGCAGCGTGCAGATC) and a reverse primer (CCATCAGTGGGCACAAGATG). PLK1 mRNA levels were normalized against GAPDH mRNA levels. Results were calculated as ΔC_T values.

2.6. Western blot analysis

The protein samples were resolved on 10% or 12% SDS-PAGE gels and were probed with the indicated antibodies. Antibodies against CDK1 and γ-tubulin were supplied by Cell Signaling Technology and Sigma-Aldrich, respectively. Antibodies against PLK1, Cdc25C and GAPDH were purchased from Santa Cruz Biotechnology.

2.7. Immunofluorescence analysis

The cells were fixed with 4% paraformaldehyde in PBS for 15 min at room temperature (for CDK1 and Cdc2C) or with methanol for 10 min at −20 °C (for γ-tubulin). Then, the cells were permeabilized with 0.25% Triton X-100 in PBS for 10 min at room temperature. After blocking with 1% BSA in PBS at room temperature for 30 min, the cells were incubated with antibodies against CDK1 or Cdc2C for 16 h at 4 °C or with the anti-γ-tubulin antibody for 40 min at room temperature. The subcellular localization of CDK1 and Cdc25C was assessed using Alexa488-conjugated anti-rabbit IgG antibody (Invitrogen) and that of γ-tubulin was analyzed using Texas red goat anti-mouse IgG antibody (Invitrogen). The cells were photographed with FluoView 1000 confocal microscopy (Olympus).

2.8. Flow cytometry analysis

The cells fixed with 70% ethanol were labeled with propidium iodide (50 μg/ml) solution containing RNase A (100 μg/ml). The

fixed cells were analyzed by flow cytometry (BD Biosciences). ModFitLT V3.0 software was used for data analysis.

3. Results

3.1. Menthol affects gene expression profile in PC-3 cells

Unsupervised hierarchical clustering analysis with all 19,741 genes obtained by RMA normalization confirmed that gene-expression profiles for all vehicle-treated replicates clustered together and that profiles for menthol-treated cells formed a separate, cohesive cluster (Fig. 1A).

3.2. Menthol modulates the expression of mitosis-related gene sets in PC-3 cells

The SAM analysis identified 5394 genes as being differentially expressed between vehicle-treated PC-3 cells and menthol-treated cells. After performing GSEA with this gene subset, we identified 28 gene sets that were down-regulated in menthol-treated cells and 6 that were up-regulated with a nominal p-value <0.05 (Supplementary Table 1, down- and up-regulated gene sets are highlighted in blue and red respectively). However, of these total 34 gene sets, only 14 had a false discovery rate (FDR) q-value <0.2 (Table 1). Twelve of these gene sets were down-regulated and two were up-regulated. Four of these gene sets are related to cell cycle processes (highlighted in bold in Table 1), two are related to the organization and biogenesis of microtubule cytoskeleton and mitochondria, and four others are related to RNA processing.

To assess the robustness of our GSEA result, we also performed GSEA analysis using all 19,741 genes. The list of significantly down- and up-regulated gene sets differed somewhat, but mitosis-related gene sets were identified regardless of whether feature selection was performed or not. Supplementary Table 2 shows the resulting list of 20 down-regulated gene sets identified in menthol-treated cells with p-value <0.05 and q-value 0.20 (Mitosis-related gene sets are highlighted in bold; no up-regulated gene set was detected at the specified significance threshold) .

3.3. PLK1 is a LES gene in the cell-cycle gene sets

We analyzed the LES or genes that contribute most to the enrichment signal in the cell cycle gene sets: CELL_CYCLE_PRO-

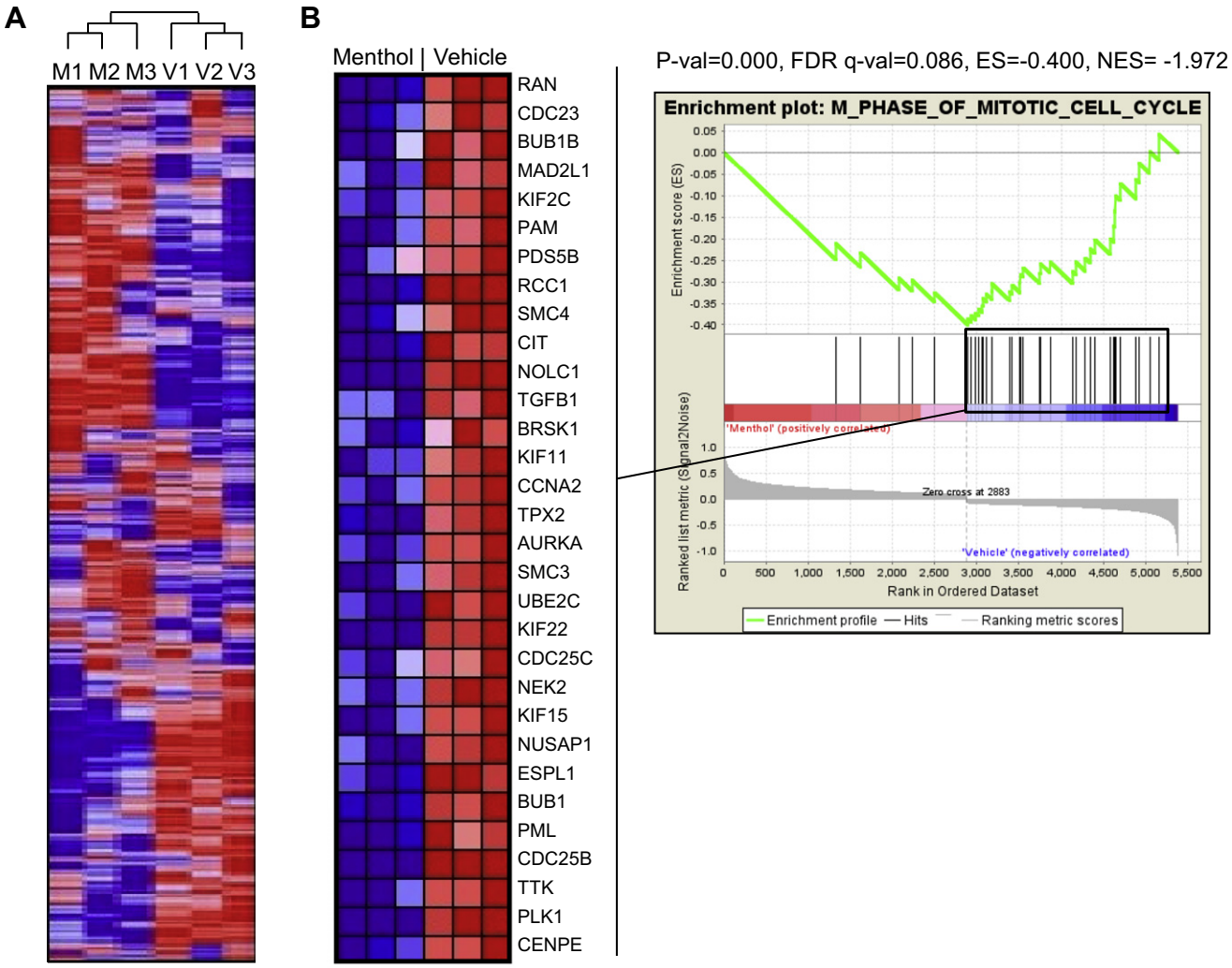

Fig. 1. Menthol affects gene expression profile in PC-3 cells. (A) Heatmap illustrating large-scale differences in gene expression between vehicle- and menthol-treated PC-3 cells. Unsupervised hierarchical clustering of gene expression profile distinguishes between menthol- and vehicle-treated PC-3 cells. Microarray experiment was triplicated in vehicle- or menthol-treated PC-3 cell groups. M, Menthol; V, Vehicle. (B) Enrichment plot by GSEA shows the distribution of up- and down-regulated M_PHASE_MITOTIC_CELL_CYCLE gene signatures between menthol- and vehicle-treated PC-3 cells. The square box indicates the LES. The heatmap view presents 31 genes of the LES. FDR, false discovery rate; ES, enrichment score; NES, normalized enrichment score. The definitions of FDR, ES, and NES are described in Table 1.

Table 1
List of 14 gene sets significantly up- or down-regulated in menthol-treated PC-3 cells.

Name[a]	ES[b]	NES[b]	NOM *p*-val[c]	FDR *q*-val[d]
MONOCARBOXYLIC_ACID_METABOLIC_PROCESS	0.510	2.070	0.000	0.047
FATTY_ACID_METABOLIC_PROCESS	0.536	1.989	0.002	0.052
MRNA_PROCESSING_GO_0006397	−0.484	−1.956	0.003	0.076
CELL_CYCLE_PROCESS	−0.321	−1.930	0.000	0.078
M_PHASE_OF_MITOTIC_CELL_CYCLE	−0.400	−1.972	0.000	0.086
RNA_PROCESSING	−0.384	−1.973	0.000	0.113
RNA_SPLICING	−0.444	−1.863	0.012	0.116
INFLAMMATORY_RESPONSE	−0.357	−1.844	0.010	0.118
MICROTUBULE_CYTOSKELETON_ORGANIZATION_AND_BIOGENESIS	−0.479	−1.791	0.011	0.123
MRNA_METABOLIC_PROCESS	−0.423	−1.792	0.012	0.135
MITOTIC_CELL_CYCLE	−0.319	−1.802	0.000	0.139
MITOSIS	−0.400	−1.989	0.006	0.147
MITOCHONDRION_ORGANIZATION_AND_BIOGENESIS	−0.470	−1.743	0.008	0.156
RESPONSE_TO_VIRUS	−0.543	−2.056	0.003	0.185

NOTE: The values of ES, NES, NOM *p*-val, and FDR *q*-val were rounded off to three decimal places. The table is sorted smallest to largest by FDR *q*-val.
[a] The four gene sets highlighted in bold are related to mitotic phase cell cycle.
[b] The normalized enrichment score (NES) for the gene set is calculated by normalizing the enrichment score (ES) across analyzed gene sets.
[c] NOM *p*-val: nominal *p*-value.
[d] FDR *q*-val: FDR corresponding to each NES is the estimated probability of false positives. FDR was represented as *q*-value, which is the analog of *p*-value that has been corrected for multiple hypothesis testing.

CESS, M_PHASE_OF_MITOTIC_CELL_CYCLE, MITOTIC_CELL_CYCLE and MITOSIS. CELL_CYCLE_PROCESS, M_PHASE_OF_MITOTIC_-CELL_CYCLE, MITOTIC_CELL_CYCLE, and MITOSIS have 65, 31, 53, and 31 LES genes, respectively. The 31 LES genes for M_PHASE_OF_MITOTIC_CELL_CYCLE and MITOSIS completely overlap with the LES genes in the CELL_CYCLE_PROCESS and MITOTIC_-CELL_CYCLE (Supplementary Table 3). Supplementary Table 4 and 5 list the LES genes for CELL_CYCLE_PROCESS and MITOTIC_-CELL_CYCLE. As an example, Fig. 1B (right) shows an enrichment plot of the distribution of up- and down-regulated genes in M_PHASE_OF_MITOTIC_CELL_CYCLE gene set between menthol and vehicle treated PC-3 cells. The heat map in Fig. 1B (left) illustrates the gene-expression patterns for the 31 LES genes.

3.4. Menthol induces G2/M arrest of PC-3 cells

As our GSEA analysis indicated that several cell-cycle gene sets were down-regulated, we postulated that menthol inhibits important cell-cycle processes in PC-3 cells. To validate this computationally driven hypothesis, we examined the cell-cycle profile in menthol-treated cells. Flow-cytometric analysis showed that the proportion of G2/M phase cells was markedly elevated in menthol-treated cells (Fig. 2A). In non-menthol treated cells, approximately 10% of cells were in G2/M phase, whereas in 2 mM menthol-treated cells, approximately 30% of cells were in G2/M phase. Because γ-tubulin is localized to centrosomes in G2/M phase through the γ-tubulin ring complex (γTuRC) [30,31], we examined the recruitment of γ-tubulin to centrosomes using immunofluorescence analysis with the anti-γ-tubulin antibody. A dot-like staining pattern, which represents localization of γ-tubulin to the centrosomes [32], was well observed in vehicle-treated cells but barely detectable in menthol-treated cells (Fig. 2B). Therefore, these results demonstrate that menthol induces G2/M arrest in PC-3 cells.

3.5. PLK1 is a plausible target for menthol action on G2/M arrest

Of the 31 LES genes presented Fig. 1B, polo-like kinase 1 (PLK1) is worthy of notice because it had the lowest *q*-value in the LES genes and was included in all four cell cycle gene sets (highlighted in bold in Supplementary Tables 3–5). PLK1 is known to mediate G2/M cell cycle progression in prostate cancer or CRPC [33,34]. PLK1 regulates the activities of various G2/M cell cycle regulators, including Cdc25C that activates the CDK1/cyclin B complex [35,36]. In addition, PLK1 controls the recruitment of the γ-tubulin

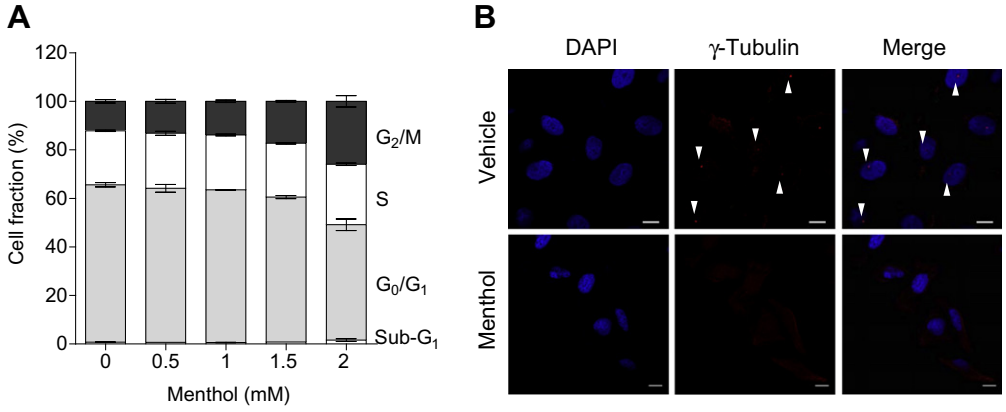

Fig. 2. Menthol induces G2/M arrest in PC-3 cells. (A) The cells were treated with menthol at the indicated concentrations for 48 h prior to flow cytometric analysis. Cell fraction is expressed as the percentage of cells in each phase of the cell cycle. The data were expressed as the mean SEM ($n = 4$). (B) The cells were treated with menthol at 2 mM for 48 h prior to immunofluorescence analysis using the anti-γ-tubulin antibody. White arrowheads indicate γ-tubulin that is recruited to centrosomes.

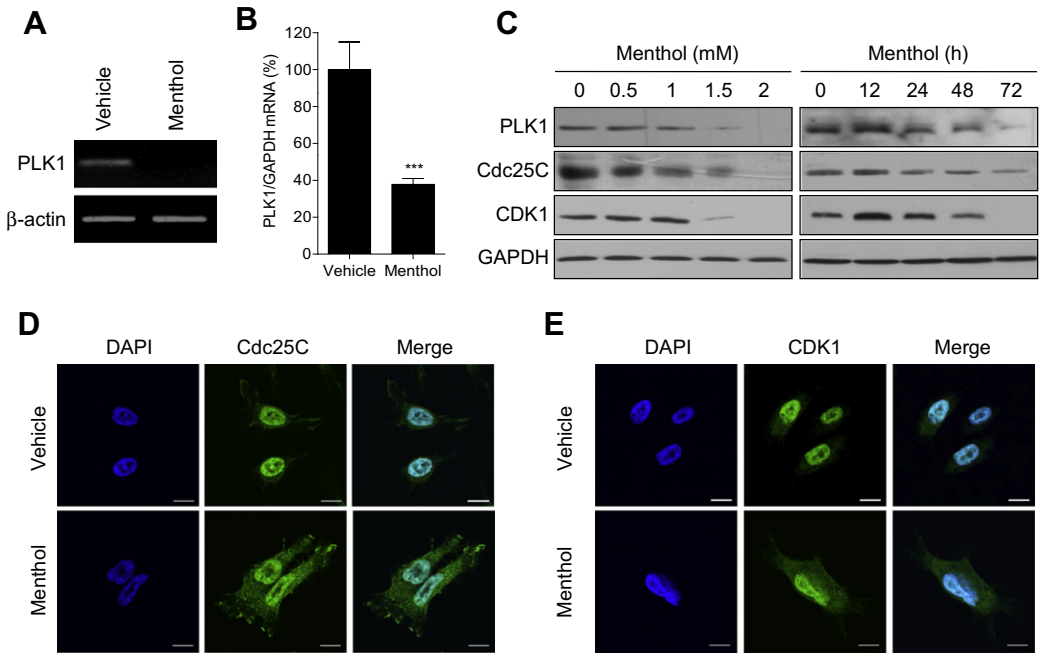

Fig. 3. Menthol down-regulates PLK1 and inhibits its downstream signaling in PC-3 cells. Cells were treated with menthol at 2 mM for 24 h prior to RT-PCR (A) or real-time RT-PCR (B) analysis. (C) Cells were treated with menthol at the indicated concentrations (left) or 2 mM (right) for 48 h (left) or the indicated times (right) prior to Western blot analysis. (D, E) The cells were treated with menthol at 2 mM for 48 h prior to immunofluorescence analysis using antibodies against Cdc25C or CDK1.

ring complex (γTuRC) to the centrosome in mitosis, a hallmark of centrosome maturation [37–39]. Therefore, we hypothesized that PLK1 plays a key role in menthol-induced G2/M arrest in PC-3 cells.

3.6. Menthol down-regulates PLK1 in PC-3 cells

To confirm that menthol down-regulates PLK1 in PC-3 cells, we performed RT-PCR analysis for PLK1. We found that menthol noticeably reduces the mRNA level of PLK1 at 24 h after treatment (Fig. 3A). To assess these results quantitatively, we performed real-time RT-PCR analysis for targeting PLK1. The analysis of PLK1 gene expression standardized to GAPDH expression revealed a significant reduction of PLK1 mRNA expression after menthol treatment compared to control (Fig. 3B). These results were further validated by Western blot analysis (Fig. 3C). Menthol decreased the protein level of PLK1 in a concentration-dependent manner. Interestingly, the protein level of Cdc25C, a PLK1 substrate, was co-reduced (Fig. 3C), which coincides with what we observed in the microarray data (highlighted in bold in Supplementary Table 3–5). Because PLK1 promotes the nuclear translocation of Cdc25C and the CDK1-Cyclin B1 complex [13–15], we performed immunofluorescence analysis using antibodies against Cdc25C and CDK1 (Fig. 3D and E). We observed that Cdc25C and CDK1 remain in the cytoplasm in menthol-treated PC-3 cells. Taken together, these results indicate that the PLK1 signaling pathways are inhibited by menthol, which suggests an underlying molecular mechanism of menthol-induced G2/M arrest.

4. Discussion

Through computationally driven hypothesis generation and experimental validation, we discovered novel insights about menthol's mechanisms of action when applied to prostate-cancer cells. Gene-expression profiling enabled us to identify genes that are up- or down-regulated in menthol-treated androgen-independent PC-3 prostate cancer cells. In this study, we described three main findings: 1) menthol produced distinct gene expression patterns that can be associated with key cellular processes, including cell-cycle regulation, 2) menthol induced G2/M arrest, and 3) menthol down-regulated PLK1 and inhibited its downstream signaling. These findings provide a biological basis for the cytotoxicity of menthol against prostate cancer cells.

As has been noted, menthol down-regulates PLK1, which is a key regulator of G2/M cell-cycle progression. Recently, PLK1 has emerged as a promising therapeutic target for prostate-cancer therapy for the following reasons: PLK1 is overexpressed in high-grade prostate cancer or CRPC [33]; overexpressed PLK1 facilitates PTEN loss–induced prostate cancer formation by attenuating mitotic stress [40]; knockdown of PLK1 induces G2/M arrest of CRPC cells [34]; and small molecule PLK1 inhibitors suppress the growth of CRPC cells [41].

Our analysis identified PLK1 as a plausible target to induce G2/M arrest in prostate cells. Menthol markedly down-regulated polo-like kinase 1 (PLK1), a key regulator of G2/M phase progression, and inhibited its downstream signaling. The results could provide a basis for future investigations that are aimed at elucidating the action of menthol on cell cycle control in prostate cancer cells.

Acknowledgments

This research was supported by the National Research Foundation of Korea (NRF) funded by the Korea government (MEST) (2009-0086652, 2010-0019472, and 2010-0021234). SRP was supported by a training fellowship from the United States National Institutes of Health (5T32CA093247).

Appendix A. Supplementary data

Supplementary data associated with this article can be found, in the online version, at http://dx.doi.org/10.1016/j.bbrc.2012.05.010.

References

[1] J.E. Damber, G. Aus, Prostate cancer, Lancet 371 (2008) 1710–1721.
[2] A. Jemal, F. Bray, M.M. Center, J. Ferlay, E. Ward, D. Forman, Global cancer statistics, CA Cancer J. Clin. (2011).

[3] B. Pang, H. Zhang, J. Wang, W.Z. Chen, S.H. Li, Q.G. Shi, R.X. Liang, B.X. Xie, R.Q. Wu, X.L. Qian, L. Yu, Q.M. Li, C.F. Huang, J.G. Zhou, Ubiquitous mitochondrial creatine kinase is overexpressed in the conditioned medium and the extract of LNCaP lineaged androgen independent cell lines and facilitates prostate cancer progression, Prostate 69 (2009) 1176–1187.
[4] M.E. Taplin, Drug insight: role of the androgen receptor in the development and progression of prostate cancer, Nat. Clin. Pract. Oncol. 4 (2007) 236–244.
[5] W.P. Harris, E.A. Mostaghel, P.S. Nelson, B. Montgomery, Androgen deprivation therapy: progress in understanding mechanisms of resistance and optimizing androgen depletion, Nat. Clin. Pract. Urol. 6 (2009) 76–85.
[6] C. Kumar-Sinha, A.M. Chinnaiyan, Molecular markers to identify patients at risk for recurrence after primary treatment for prostate cancer, Urology 62 (2003) 19–35.
[7] D. Talantov, T.A. Jatkoe, M. Bohm, Y. Zhang, A.M. Ferguson, P.D. Stricker, M.W. Kattan, R.L. Sutherland, J.G. Kench, Y. Wang, S.M. Henshall, Gene based prediction of clinically localized prostate cancer progression after radical prostatectomy, J. Urol. 184 (2010) 1521–1528.
[8] S. Varambally, J. Yu, B. Laxman, D.R. Rhodes, R. Mehra, S.A. Tomlins, R.B. Shah, U. Chandran, F.A. Monzon, M.J. Becich, J.T. Wei, K.J. Pienta, D. Ghosh, M.A. Rubin, A.M. Chinnaiyan, Integrative genomic and proteomic analysis of prostate cancer reveals signatures of metastatic progression, Cancer Cell 8 (2005) 393–406.
[9] G.V. Glinsky, A.B. Glinskii, A.J. Stephenson, R.M. Hoffman, W.L. Gerald, Gene expression profiling predicts clinical outcome of prostate cancer, J. Clin. Invest. 113 (2004) 913–923.
[10] J.H. Luo, Gene expression alterations in human prostate cancer, Drugs Today (Barc) 38 (2002) 713–719.
[11] Y.P. Yu, D. Landsittel, L. Jing, J. Nelson, B. Ren, L. Liu, C. McDonald, R. Thomas, R. Dhir, S. Finkelstein, G. Michalopoulos, M. Becich, J.H. Luo, Gene expression alterations in prostate cancer predicting tumor aggression and preceding development of malignancy, J. Clin. Oncol. 22 (2004) 2790–2799.
[12] L.H. Stockwin, B. Han, S.X. Yu, M.G. Hollingshead, M.A. ElSohly, W. Gul, D. Slade, A.M. Galal, D.L. Newton, M.A. Bumke, Artemisinin dimer anticancer activity correlates with heme-catalyzed reactive oxygen species generation and endoplasmic reticulum stress induction, Int. J. Cancer 125 (2009) 1266–1275.
[13] Y. Li, A. Mizokami, K. Izumi, K. Narimoto, T. Shima, J. Zhang, J. Dai, E.T. Keller, M. Namiki, CTEN/tensin 4 expression induces sensitivity to paclitaxel in prostate cancer, Prostate 70 (2010) 48–60.
[14] T. Patel, Y. Ishiuji, G. Yosipovitch, Menthol: a refreshing look at this ancient compound, J. Am. Acad. Dermatol. 57 (2007) 873–878.
[15] R. Wondergem, T.W. Ecay, F. Mahieu, G. Owsianik, B. Nilius, HGF/SF and menthol increase human glioblastoma cell calcium and migration, Biochem. Biophys. Res. Commun. 372 (2008) 210–215.
[16] S.H. Kim, J.H. Nam, E.J. Park, B.J. Kim, S.J. Kim, I. So, J.H. Jeon, Menthol regulates TRPM8-independent processes in PC-3 prostate cancer cells, Biochim. Biophys. Acta 1792 (2009) 33–38.
[17] V. Copois, F. Bibeau, C. Bascoul-Mollevi, N. Salvetat, P. Chalbos, C. Bareil, L. Candeil, C. Fraslon, E. Conseiller, V. Granci, P. Maziere, A. Kramar, M. Ychou, B. Pau, P. Martineau, F. Molina, M. Del Rio, Impact of RNA degradation on gene expression profiles: assessment of different methods to reliably determine RNA quality, J. Biotechnol. 127 (2007) 549–559.
[18] S. Weis, I.C. Llenos, J.R. Dulay, M. Elashoff, F. Martinez-Murillo, C.L. Miller, Quality control for microarray analysis of human brain samples: The impact of postmortem factors, RNA characteristics, and histopathology, J. Neurosci. Methods 165 (2007) 198–209.
[19] J. Brettschneider, F. Collin, B.M. Bolstad, T.P. Speed, Quality assessment for short oligonucleotide microarray data, Technometrics 50 (2008) 241–264.
[20] S.H. Guan, J. Zheng, J. Brettschneider, Microarray data quality assessment for developmental time series, Syst. Biol. Stat. Bioinf. (2007) 79–82.
[21] B. Bolstad, F. Collin, J. Brettschneider, K. Simpson, L. Cope, R. Irizarry, T. Speed, Quality assessment of Affymetrix GeneChip data, Bioinf. Comput. Biol. Solutions Using R and Bioconductor (2005) 33–47.
[22] H. Bengtsson, K. Simpson, J. Bullard, K. Hansen, aroma. affymetrix: A Generic Framework in R for Analyzing Small to Very Large Affymetrix Data Sets in Bounded Memory, Department of Statistics, Berkeley, 2008.
[23] B.M. Bolstad, R.A. Irizarry, M. Astrand, T.P. Speed, A comparison of normalization methods for high density oligonucleotide array data based on variance and bias, Bioinformatics 19 (2003) 185–193.
[24] M. Dai, P. Wang, A.D. Boyd, G. Kostov, B. Athey, E.G. Jones, W.E. Bunney, R.M. Myers, T.P. Speed, H. Akil, Evolving gene/transcript definitions significantly alter the interpretation of GeneChip data, Nucleic Acids Res. 33 (2005) e175.
[25] M. Reich, T. Liefeld, J. Gould, J. Lerner, P. Tamayo, J.P. Mesirov, GenePattern 2.0, Nat. Genet. 38 (2006) 500–501.
[26] V.G. Tusher, R. Tibshirani, G. Chu, Significance analysis of microarrays applied to the ionizing radiation response, Proc. Natl. Acad. Sci. USA 98 (2001) 5116–5121.
[27] A. Subramanian, P. Tamayo, V.K. Mootha, S. Mukherjee, B.L. Ebert, M.A. Gillette, A. Paulovich, S.L. Pomeroy, T.R. Golub, E.S. Lander, J.P. Mesirov, Gene set enrichment analysis: a knowledge-based approach for interpreting genome-wide expression profiles, Proc. Natl. Acad. Sci. USA 102 (2005) 15545–15550.
[28] A. Subramanian, H. Kuehn, J. Gould, P. Tamayo, J.P. Mesirov, GSEA-P: a desktop application for Gene Set Enrichment Analysis, Bioinformatics 23 (2007) 3251–3253.
[29] S.H. Kim, S.Y. Kim, E.J. Park, J. Kim, H.H. Park, I. So, S.J. Kim, J.H. Jeon, Icilin induces G1 arrest through activating JNK and p38 kinase in a TRPM8-independent manner, Biochem. Biophys. Res. Commun. 406 (2011) 30–35.
[30] E. Schiebel, Gamma-tubulin complexes: binding to the centrosome, regulation and microtubule nucleation, Curr. Opin. Cell Biol. 12 (2000) 113–118.
[31] W.C. Zimmerman, J. Sillibourne, J. Rosa, S.J. Doxsey, Mitosis-specific anchoring of gamma tubulin complexes by pericentrin controls spindle organization and mitotic entry, Mol. Biol. Cell 15 (2004) 3642–3657.
[32] L. Haren, T. Stearns, J. Luders, Plk1-dependent recruitment of gamma-tubulin complexes to mitotic centrosomes involves multiple PCM components, PLoS One 4 (2009) e5976.
[33] W. Weichert, M. Schmidt, V. Gekeler, C. Denkert, C. Stephan, K. Jung, S. Loening, M. Dietel, G. Kristiansen, Polo-like kinase 1 is overexpressed in prostate cancer and linked to higher tumor grades, Prostate 60 (2004) 240–245.
[34] S. Reagan-Shaw, N. Ahmad, Silencing of polo-like kinase (Plk) 1 via siRNA causes induction of apoptosis and impairment of mitosis machinery in human prostate cancer cells: implications for the treatment of prostate cancer, FASEB J. 19 (2005) 611–613.
[35] M.A. van Vugt, R.H. Medema, Getting in and out of mitosis with Polo-like kinase-1, Oncogene 24 (2005) 2844–2859.
[36] F.A. Barr, H.H. Sillje, E.A. Nigg, Polo-like kinases and the orchestration of cell division, Nat. Rev. Mol. Cell Biol. 5 (2004) 429–440.
[37] H.A. Lane, E.A. Nigg, Antibody microinjection reveals an essential role for human polo-like kinase 1 (Plk1) in the functional maturation of mitotic centrosomes, J. Cell Biol. 135 (1996) 1701–1713.
[38] I. Sumara, J.F. Gimenez-Abian, D. Gerlich, T. Hirota, C. Kraft, C. de la Torre, J. Ellenberg, J.M. Peters, Roles of polo-like kinase 1 in the assembly of functional mitotic spindles, Curr. Biol. 14 (2004) 1712–1722.
[39] L. Haren, T. Stearns, J. Luders, Plk1-dependent recruitment of gamma-tubulin complexes to mitotic centrosomes involves multiple PCM components, PLoS One 4 (2009) e5976–5985.
[40] X.S. Liu, B. Song, B.D. Elzey, T.L. Ratliff, S.F. Konieczny, L. Cheng, N. Ahmad, X. Liu, Polo-like kinase 1 facilitates loss of Pten tumor suppressor-induced prostate cancer formation, J. Biol. Chem. 286 (2011) 35795–35800.
[41] K. Strebhardt, A. Ullrich, Targeting polo-like kinase 1 for cancer therapy, Nat. Rev. Cancer 6 (2006) 321–330.